

Cite this: *Dalton Trans.*, 2018, **47**, 16264

Cooperative metal–ligand influence on the formation of coordination polymers, and conducting and photophysical properties of Tl(I) β -oxodithioester complexes†‡

Chote Lal Yadav,^a Gunjan Rajput,^b Krishna K. Manar,^a Kavita Kumari,^a Michael G. B. Drew^c and Nanhai Singh *^a

Eight novel Tl(I) β -oxodithioester complexes, [Tl]_n (**1–8**), with ligands, L = methyl-3-hydroxy-3-(2-furyl)-2-propenedithioate (L1), methyl-3-hydroxy-3-(2-thienyl)-2-propenedithioate (L2), methyl-3-hydroxy-3-(3-pyridyl)-2-propenedithioate (L3), methyl-3-hydroxy-3-(4-pyridyl)-2-propenedithioate (L4), methyl-3-hydroxy-3-(9-anthracenyl)-2-propenedithioate (L5), methyl-3-hydroxy-3-(4-fluorophenyl)-2-propenedithioate (L6), methyl-3-hydroxy-3-(4-chlorophenyl)-2-propenedithioate (L7) and methyl-3-hydroxy-3-(4-bromophenyl)-2-propenedithioate (L8), were synthesized and thoroughly characterized by elemental analysis, and IR, UV-Vis, ¹H and ¹³C{¹H} NMR spectroscopy, and their structures were ascertained by X-ray crystallography. Complexes **1** and **2** crystallized in *P*2₁ and *P*2₁2₁2₁ chiral space groups, respectively, and were studied using Circular Dichroism (CD) spectra. Solid state structural analyses revealed that the β -oxodithioester ligands are bonded to Tl(I) ions in (O, S) chelating and chelating–bridging modes, thereby forming different types of 1D and 2D coordination polymeric structures. By considering the metal-assisted bonding interactions, various coordination numbers of 5–8 and 10 are established around the metal centre. Except for **5** and **7a** which have Tl...Tl separations at 3.724(1) and 3.767(1), 3.891(1) Å respectively, the remaining complexes have no Tl...Tl distances <4.0 Å. This indicates that the majority of structures contain only weak inter- and intra-molecular thalophilic interactions. The structures of **1–8** highlight the role played by variations in substituents in the dithioester unit in the structure and properties of the complexes. The multi-dimensional assembly in these complexes rests on important non-covalent C–H... π (TIOSC₃, chelate), C–H...X (X = F, Cl, O, N), C–H... π , H...H and rare Tl...H–C intermolecular anagostic interactions. The Tl...H–C anagostic interactions together with C–O...Tl and C–S...Tl interactions formed 7-, 11- and 12-membered chelate rings about the metal centers. The anagostic interactions in **1**, **2** and **7b** were assessed by theoretical calculations. All the complexes showed bright green luminescent emissions in solution and solid phases. Time-resolved emission spectra revealed a triexponential decay curve and short mean lifetime for fluorescence behavior.

Received 12th September 2018,
Accepted 12th October 2018

DOI: 10.1039/c8dt03694b

rsc.li/dalton

Introduction

Considerable attention has been devoted in recent years to the synthesis of coordination polymers of transition metals with

unusual structures and properties due to their interesting topologies and potential applications in optical, photo-, molecular electrical and magnetic materials.^{1–5} In spite of their important optical and conducting properties and varied appli-

^aDepartment of Chemistry, Institute of Science, Banaras Hindu University, Varanasi-221005, India. E-mail: nsinghbhu@gmail.com, nsingh@bhu.ac.in

^bDepartment of Chemistry, Ram Chandra Uniyal Government PG College, Uttarkashi-249193, India

^cDepartment of Chemistry, University of Reading, Whiteknights, Reading RG6 6AD, UK
† Part of the work was presented at ISACS: Challenges in Inorganic Chemistry, April 10–13, 2017, Manchester, UK.

‡ Electronic supplementary information (ESI) available: S1: Simulated and experimental PXRD patterns for **1–8**; Fig. S1: Simulated and experimental PXRD patterns for **1–8**; Fig. S2: (a) UV-Vis spectra of complexes as solid in nujol mull; (b) and (c) their emission spectra in the solid phase; Fig. S3: Non-covalent inter-

actions in **3**, **4**, **6** and **7b**; Fig. S4: Temperature dependent pressed pellet conductivity plots for complexes **1–8**; Fig. S5: Solid state CD spectra of complexes **1** and **2**; Table S1: Crystallographic parameters for the ligand L5 and complexes **1–8**; Table S2: Selected bond lengths (Å) and angles (°) for complexes **1–4**, **7b** and **8**; Table S3: Selected bond lengths (Å) and angles (°) for complex **5**; Table S4: Selected bond lengths (Å) and angles (°) for complex **6**; Table S5: Selected bond lengths (Å) and angles (°) for complexes **7a**; Table S6: Intermolecular interactions of note in **3**, **4** and **6**, distances (Å) and angles (°). CCDC 1534939, 1534940, 1842767, 1566019, 1534943, 1534941, 1534942, 1842768, 1566020 and 1842769. For ESI and crystallographic data in CIF or other electronic format see DOI: 10.1039/c8dt03694b

cations in materials chemistry and medical technology, coordination polymers of low valence p-block (Tl, Sn, and Pb) metal ions with organic ligands including thiolato ligands have received very little attention.^{6–10}

Transition and main group metal dithiolates have been extensively studied because of their rich structural diversity and myriad applications.^{11,12} Complexes of thallium with 1,1-dithioligands including dithiocarbamate having identical (S, S) donor atoms have been known for many years.⁸ Transition metal complexes of somewhat similar β -oxodithioester ligands with (O, S) hetero donor atoms have been sporadically reported.¹³ In comparison, despite their synthetic versatility and practical applications, Tl(I) β -oxodithioester complexes have not been investigated until recently.

Bearing these points in mind we were motivated to undertake the investigation of the synthesis, crystal structures, and luminescent and conducting properties of some novel Tl(I) coordination polymers derived from potassium salts of functionalized β -oxodithioester ligands (Scheme 1). The important aspects of this work are: (i) the β -oxodithioesters display (O, S) coordination and electron delocalization over the stable 6-membered chelate ring about the metal center. In comparison, the previously reported 1,1-dithiolates including dithiocarbamates form strained 4-membered chelate rings *via* identical (S, S) donor atoms. This difference in behavior may result in huge differences in their structure/bonding and physico-chemical properties; (ii) the small and hard O atom having no d orbitals and a distinctly soft character together with larger S with more diffused p and d orbitals in the dithioester unit lead to greater affinity for the large Tl(I) ion which lies in between the hard and soft Lewis acids since its size and charge are comparable to a hard K^+ alkali metal ion and a soft

Ag^+ coinage metal ion. Furthermore, the presence of a stereochemically active $6s^2$ lone pair with greater relativistic effects may induce the formation of coordination polymers through Tl–O and Tl–S bonds with varied polarity and stability; (iii) a systematic variation in the steric and electronic properties and the presence of additional donor atoms (N, O, S, F, Cl, and Br) on the substituents may facilitate the generation of intra- and intermolecular non-covalent and rare Tl...H–C anagostic and Tl...Tl metallophilic interactions in the organization of multi-dimensional assembly and (iv) the Tl(I) chromophore in the extended rigid coordination polymeric structures and in part metallophilic interactions may lead to enhanced luminescent and conducting properties of the complexes. Theoretical calculations were performed to support the rare Tl...H–C intermolecular anagostic interactions. Impressive photoluminescence, lifetime measurements and semiconducting characteristics of the complexes are also described in this contribution. Significant differences in the structural features of these complexes with those of previously reported⁸ Tl(I) dithiocarbamates are studied.

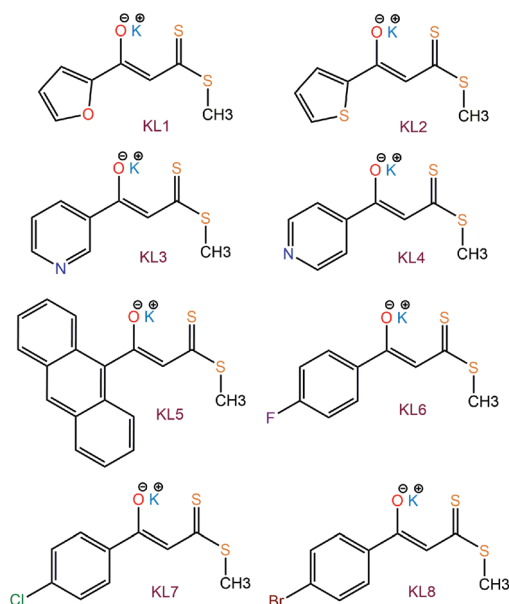
Experimental section

General methods and materials

All the reactions were carried out in open air at ambient temperature. The solvents were purified by standard procedures and where necessary dried before use. All the commercially available reagents, $TlNO_3$, 2-acetylfuran, 2-acetylthiophene (all from Sigma-Aldrich), 3-acetylpyridine, 4-acetylpyridine, 9-acetylanthracene (SPECTROCHEM), *p*-fluoroacetophenone, *p*-chloroacetophenone and *p*-bromoacetophenone (Avra Synthesis) were used as received without further purification. Experimental details of the elemental analysis (C, H, and N) and recording of FT IR (as KBr discs), and 1H and $^{13}C\{^1H\}$ NMR in $CDCl_3$ /DMSO- d_6 on a JEOL ECZ500 MHz FT NMR spectrometer of the ligands L1–L8 and complexes 1–8 have been described earlier.^{8,13d} $(CH_3)_4Si$ (TMS) was used as an internal standard for recording NMR spectra. CD spectra were collected on a JASCO J-815 spectrophotometer. Diffuse reflectance, UV-visible absorption, and solution and solid phase emission spectra were obtained using a Harrick Praying Mantis accessory on Shimadzu UV-3600, Shimadzu UV-1800 and Fluorolog Horiba Jobin Yvon/PerkinElmer LS-55 fluorescence spectrophotometers, respectively, at room temperature. Fluorescence decay lifetimes were recorded on an Edinburgh OB920 Fluorescence Spectrometer. The pressed pellet temperature dependent conductivity measurement was carried out on a Keithley 236 source measure unit. The details on single crystal X-ray data are provided in the crystal discussion section and X-ray powder diffraction data were collected using a Rigaku MultiFlex-600 system with Cu- $K\alpha$ radiation ($\lambda = 1.54056 \text{ \AA}$) with a scan rate of 2° min^{-1} in the range $2\theta = 5\text{--}50^\circ$.

Synthesis of ligands (L1–L8)

The ligands methyl-3-hydroxy-3-(2-furyl)-2-propenedithioate (L1), methyl-3-hydroxy-3-(2-thienyl)-2-propenedithioate (L2),



Scheme 1 Potassium salts (KL1–KL8) of β -oxodithioester ligands used in this work.

methyl-3-hydroxy-3-(3-pyridine)-2-propenedithioate (L3), methyl-3-hydroxy-3-(4-pyridyl)-2-propenedithioate (L4), methyl-3-hydroxy-3-(9-anthracenyl)-2-propenedithioate (L5), methyl-3-hydroxy-3-(*p*-fluorophenyl)-2-propenedithioate (L6), methyl-3-hydroxy-3-(*p*-chlorophenyl)-2-propenedithioate (L7) and methyl-3-hydroxy-3-(*p*-bromophenyl)-2-propenedithioate (L8) and their potassium salts were prepared adopting previously reported methods^{13d} (Scheme 2). To a solution of NaH (0.6 g, 25 mmol) dissolved in a DMF:hexane mixture (4:1; 20 mL) was added (dropwise) 2-acetyl furan (1.10 g, 10.0 mmol) (for L1), 2-acetylthiophene (1.26 g, 10.0 mmol) (for L2), 3-acetylpyridine (1.20 g, 10.0 mmol) (for L3), 4-acetylpyridine (1.21 g, 10.0 mmol) (for L4), 9-acetylanthracene (2.20 g, 10.0 mmol) (for L5), *p*-fluoroacetophenone (1.38 g, 10.0 mmol) (for L6), *p*-chloroacetophenone (1.54 g, 10.0 mmol) (for L7) or *p*-bromoacetophenone (1.99 g, 10 mmol) (for L8) in DMF (20 mL) separately. After stirring for 1 h in an ice bath under a N₂ atmosphere, a solution of dimethyltrithiocarbonate (TTC)¹⁴ (1.38 g, 10 mmol) was added slowly and the mixture was additionally stirred for another 10 h at room temperature. Excess NaH was neutralized by adding 0.1 M HCl (50 mL), and the product was extracted with dichloromethane (3 × 50 mL), washed with brine solution and water, concentrated and dried over anhydrous Na₂SO₄. The product was purified by silica gel (100–200 mesh) chromatography using hexane as the eluent to collect crystalline yellow solids (for characterization data for L1–L8, see S1, ESI†).

Syntheses of complexes 1–8

For the syntheses of complexes, potassium salts of the ligands KL1–KL8 were obtained by the following procedure. To a stirred 10 mL acetone solution of ligands L1 (0.22 g, 1 mmol), L2 (0.20 g, 1 mmol), L3 (0.21 g, 1 mmol), L4 (0.21 g, 1 mmol), L5 (0.31 g, 1 mmol), L6 (0.24 g, 1 mmol), L7 (0.23 g, 1 mmol) and L8 (0.29 g, 1 mmol) was added solid K₂CO₃ (0.21 g, 1.5 mmol) separately and in each case the reaction mixture was additionally stirred for 4–5 h under reflux conditions. The

solution was cooled, filtered off and dried using a vacuum evaporator to yield the potassium salts of the ligands KL1–KL8 as yellow to orange solid products.

The complexes were obtained adopting the following general procedure. To a 15 mL stirred methanol solution of the potassium salt of the ligand KL1 (0.24 g, 1 mmol), KL2 (0.25 g, 1 mmol), KL3 (0.25 g, 1 mmol), KL4 (0.25 g, 1 mmol), KL5 (0.35 g, 1 mol), KL6 (0.27 g, 1 mmol), KL7 (0.28 g, 1 mmol) or KL8 (0.35 g, 1 mmol) was gradually added a 10 mL methanol:water (80:20) solution of TiNO₃ (0.27 g, 1 mmol) and further stirred for 4–6 h. The reddish-brown solid formed was filtered off, washed with methanol, dried in open air and dissolved in DMF to yield red-orange crystals within 10 days.

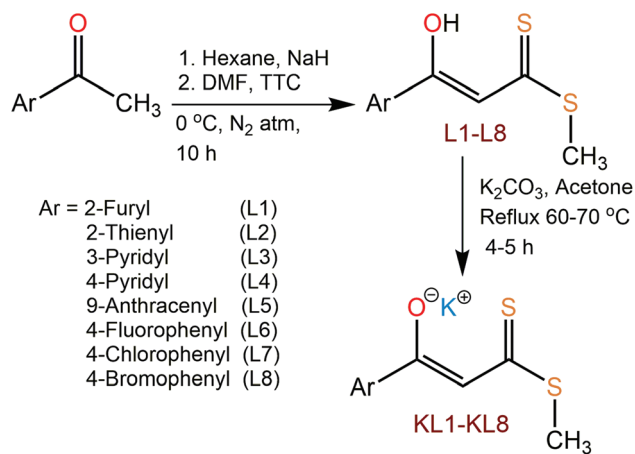
Characterization data

1 Yield: (0.314 g, 78%). M. P.: 172–175 °C. Anal. calcd for C₈H₇O₂TiS₂ (403.65): C 23.40, H 3.44%. Found: C 23.25, H 3.48%. IR (KBr, cm⁻¹): 1590 (ν_{C=O}), 1565 (ν_{C=C}), 1009 (ν_{C=S}). ¹H NMR (500.15 MHz, DMSO-*d*₆, ppm): δ 2.30 (s, 3H, -SCH₃), 6.45 (s, 1H, -CH=C-), 6.75–7.62 (m, 3H, C₄H₃O). ¹³C{¹H} NMR (125.03 MHz, DMSO-*d*₆, ppm) δ 17.82 (-SCH₃), 111.08 (-CH=C-), 112.05, 113.39, 143.88, 156.80 (C₄H₃O), 169.08 (=C-O-), 195.03 (-C=S). UV-Vis (DMSO, λ_{max} (nm), ε (M⁻¹ cm⁻¹)): 315 (1.52 × 10³), 405 (1.25 × 10⁴); (Nujol, λ_{max} (nm)): 292, 352 and 418.

2 Yield: (0.339 g, 81%). M. P.: 138–142 °C. Anal. calcd for C₈H₇OTiS₃ (419.71): C 22.89, H 1.68%. Found: C 22.58, H 1.65%. IR (KBr, cm⁻¹): 1578 (ν_{C=O}), 1516 (ν_{C=C}), 1020 (ν_{C=S}). ¹H NMR (500.15 MHz, DMSO-*d*₆, ppm): δ 2.30 (s, 3H, -SCH₃), 6.97 (s, 1H, -CH=C-), 7.01–7.72 (m, 3H, C₄H₃S). ¹³C{¹H} NMR (125.03 MHz, DMSO-*d*₆, ppm) δ 17.94 (-SCH₃), 113.29 (-CH=C-), 126.79, 128.32, 129.64, 150.37 (C₄H₃S), 172.80 (=C-O-), 193.34 (-C=S). UV-Vis (DMSO, λ_{max} (nm), ε (M⁻¹ cm⁻¹)): 355 (6.24 × 10³), 413 (0.62 × 10⁴); (Nujol, λ_{max} (nm)): 296, 354 and 502.

3 Yield: (0.286 g, 69%). M. P.: 132–136 °C. Anal. calcd for C₉H₈NOTiS₂ (414.68): C 26.07, H 1.94, N 3.38%. Found: C 25.85, H 1.95, N 3.35%. IR (KBr, cm⁻¹): 1595 (ν_{C=O}), 1534 (ν_{C=C}), 1024 (ν_{C=S}). ¹H NMR (500.15 MHz, DMSO-*d*₆, ppm): δ 2.62 (s, 3H, -SCH₃), 7.21 (s, 1H, -CH=C-), 7.51, 8.22, 8.67, 9.05 (m, 4H, C₅H₄N). ¹³C{¹H} NMR (125.03 MHz, DMSO-*d*₆, ppm) δ 17.67 (-SCH₃), 113.35 (-CH=C-), 123.42, 134.39, 136.94, 148.30, 150.23 (C₅H₄N), 176.77 (=C-O-), 195.13 (-C=S). UV-Vis (DMSO, λ_{max} (nm), ε (M⁻¹ cm⁻¹)): 352 (9.11 × 10³), 398 (1.40 × 10⁴); (Nujol, λ_{max} (nm)): 287, 352 and 472.

4 Yield: (0.315 g, 76%). M. P.: 157–160 °C. Anal. calcd for C₉H₈NOTiS₂ (414.65): C 26.05, H 1.94, N 3.23%. Found: C 25.90, H 2.05, N 3.30%. IR (KBr, cm⁻¹): 1594 (ν_{C=O}), 1512 (ν_{C=C}), 1060 (ν_{C=S}). ¹H NMR (500.15 MHz, DMSO-*d*₆, ppm): δ 2.33 (s, 3H, -SCH₃), 7.03 (s, 1H, -CH=C-), 7.60–8.53 (m, 4H, C₅H₄N). ¹³C{¹H} NMR (125.03 MHz, DMSO-*d*₆, ppm) δ 18.03 (-SCH₃), 113.64 (-CH=C-), 121.42, 149.56, 150.26 (C₅H₄N), 175.95 (=C-O-), 198.95 (-C=S). UV-Vis (DMSO, λ_{max} (nm), ε (M⁻¹ cm⁻¹)): 323 (2.55 × 10³), 415 (1.42 × 10⁴); (Nujol, λ_{max} (nm)): 295, 355 and 530.



Scheme 2 General methodology for the synthesis of ligands L1–L8 and their potassium salts KL1–KL8.

5 Yield: (0.349 g, 68%). M. P.: 219–223 °C. Anal. calcd for $C_{18}H_{13}OTIS_2$ (513.80): C 42.08, H 2.55%. Found: C 41.88, H 2.62%. IR (KBr, cm^{-1}): 1559 (ν_{C-O}), 1519 ($\nu_{C=C}$), 1002 (ν_{C-S}). 1H NMR (500.15 MHz, DMSO- d_6 , ppm): δ 2.41 (s, 3H, $-SCH_3$), 6.55 (s, 1H, $-CH=C-$), 7.41–8.43 (m, 9H, $C_{14}H_9$). $^{13}C\{^1H\}$ NMR (125.03 MHz, DMSO- d_6 , ppm) δ 17.79 ($-SCH_3$), 116.37 ($-CH=C-$), 125.58, 125.69, 125.77, 127.07, 127.50, 128.61, 131.43, 141.76 ($C_{14}H_9$), 177.83 ($=C-O-$), 194.87 ($-C=S$). UV-Vis (DMSO, λ_{max} (nm), ϵ ($M^{-1} cm^{-1}$)): 310 (2.85×10^3), 380 (1.14×10^4); (Nujol, λ_{max} (nm)): 295, 345 and 477.

6 Yield: (0.323 g, 75%). M. P.: 143–147 °C. Anal. calcd for $C_{10}H_8FOTIS_2$ (431.67): C 27.82, H 1.87%. Found: C 27.78, H 1.92%. IR (KBr, cm^{-1}): 1598 (ν_{C-O}), 1505 ($\nu_{C=C}$), 1010 (ν_{C-S}). 1H NMR (500.15 MHz, DMSO- d_6 , ppm): δ 2.34 (s, 3H, $-SCH_3$), 6.74 (s, 1H, $-CH=C-$), 7.15–7.85 (m, 4H, C_6H_4F). $^{13}C\{^1H\}$ NMR (125.03 MHz, DMSO- d_6 , ppm) δ 18.05 ($-SCH_3$), 113.70 ($-CH=C-$), 125.37, 129.81, 130.31, 138.53 (C_6H_4F), 178.66 ($=C-O-$), 192.15 ($-C=S$). UV-Vis (DMSO, λ_{max} (nm), ϵ ($M^{-1} cm^{-1}$)): 315 (0.26×10^4), 400 (1.67×10^4); (Nujol, λ_{max} (nm)): 292, 345 and 492.

7 Yield: (0.313 g, 70%). M. P.: 164–168 °C. Anal. calcd for $C_{10}H_8ClOTIS_2$ (448.13): C 26.80, H 1.80%. Found: C 26.76, H 1.93%. IR (KBr, cm^{-1}): 1588 (ν_{C-O}), 1490 ($\nu_{C=C}$), 1011 (ν_{C-S}). 1H NMR (500.15 MHz, DMSO- d_6 , ppm): δ 2.30 (s, 3H, $-SCH_3$), 7.04 (s, 1H, $-CH=C-$), 7.35–7.74 (m, 4H, C_6H_4Cl). $^{13}C\{^1H\}$ NMR (125.03 MHz, DMSO- d_6 , ppm) δ 17.40 ($-SCH_3$), 112.97 ($-CH=C-$), 127.89, 128.57, 133.91, 140.86 (C_6H_4Cl), 176.77 ($=C-O-$), 195.20 ($-C=S$). UV-Vis (DMSO, λ_{max} (nm), ϵ ($M^{-1} cm^{-1}$)): 322 (1.45×10^3), 405 (9.48×10^3); (Nujol, λ_{max} (nm)): 291, 345 and 475.

8 Yield: (0.359 g, 73%). M. P.: 166–170 °C. Anal. calcd for $C_{10}H_8BrOTIS_2$ (492.59): C 24.38, H 1.64%. Found: C 26.33, H 1.75%. IR (KBr, cm^{-1}): 1583 (ν_{C-O}), 1488 ($\nu_{C=C}$), 1006 (ν_{C-S}). 1H NMR (500.15 MHz, DMSO- d_6 , ppm): δ 2.35 (s, 3H, $-SCH_3$), 7.09 (s, 1H, $-CH=C-$), 7.54–7.73 (m, 4H, C_6H_4Br). $^{13}C\{^1H\}$ NMR (125.03 MHz, DMSO- d_6 , ppm) δ 17.97 ($-SCH_3$), 113.48 ($-CH=C-$), 123.36, 129.42, 131.38, 141.75 (C_6H_4Br), 177.42 ($=C-O-$), 195.73 ($-C=S$). UV-Vis (DMSO, λ_{max} (nm), ϵ ($M^{-1} cm^{-1}$)): 315 (1.44×10^3), 406 (1.20×10^4); (Nujol, λ_{max} (nm)): 288, 346 and 502.

Theoretical calculations

Single point calculations were carried out using the Gaussian 03 program.¹⁵ Structures were investigated using the B3LYP density functional together with basis sets LANL2DZ for Tl, 6-31+G* for S and 6-31G for the remaining atoms. Models were taken from the crystal structures but with hydrogen atoms given theoretical positions.

X-ray structure determination

Single crystal X-ray diffraction data for the ligand L5 and complexes **2** and **5–8** were collected on an Oxford Diffraction X-Calibur CCD diffractometer using Mo K α radiation at 150 K; **1** and **3** on a Bruker D8 Quest SCM X-ray diffractometer at 100 K and **4** on a Bruker AXS D8 Quest SC X-ray diffractometer at 295 K. Data reduction for L5 and **1–8** was carried out using

the CrysAlis program.¹⁶ The structures were solved by direct methods using SHELXS-97¹⁷ and refined on F^2 by the full matrix least squares technique using SHELXL2016-6.¹⁸ Non-hydrogen atoms were refined anisotropically and hydrogen atoms were geometrically fixed with thermal parameters equivalent to 1.2 times that of the atom to which they were bonded. In **7b** the phenyl ring is disordered and two orientations were refined with occupancies x and $1 - x$. Diagrams for ligand L5 and all complexes were obtained using OLEX2,^{19a} Diamond^{19b} and Mercury^{19c} software. Crystallographic data for **1–8** and L5 were deposited at the Cambridge Crystallographic Data Centre with reference numbers CCDC 1534939, 1534940, 1842767, 1566019, 1534943, 1534941, 1534942, 1842768, 1566020 and 1842769, respectively.†

Results and discussion

Synthesis and characterization

The reactions of a methanol–water solution of $TlNO_3$ and methanolic solutions of potassium salts of the β -oxodithioester ligands, KL1–KL8, in an equimolar ratio afforded the formation of air and moisture stable homoleptic complexes $[Tl]_n$ **1–8** in good yields. All the complexes were insoluble in water and sparingly soluble in common organic solvents such as dichloromethane, acetone, acetonitrile, ethanol and methanol but soluble in DMSO and DMF due to their polymeric nature. They were characterized by elemental analysis, and IR, UV-Vis, 1H and $^{13}C\{^1H\}$ NMR spectroscopy. Solid state structural determination by X-ray crystallography revealed their spectacular 1D and 2D coordination polymeric structures displaying $Tl \cdots Tl$ and rare $Tl \cdots H-C$ intermolecular anagostic interactions along with various interesting non-covalent interactions. The anagostic interactions in **1**, **2** and **7b** were corroborated by theoretical calculations. The semiconducting behaviors of the complexes were investigated using diffuse reflectance spectra. The phase purity of the bulk products **1–8** was assessed by a comparison of the experimental PXRD patterns with their respective simulated powder patterns obtained from the single crystal data. The experimental and simulated PXRD patterns matched well indicating the phase purity of the bulk samples (Fig. S1, ESI†). All the complexes showed bright green luminescence characteristics in solution and solid phases; also the luminescence lifetime decay profiles were studied. Complexes **1** and **2** are chiral as confirmed by the CD spectra.

Spectroscopic characterization

In the IR spectra, complexes **1–8** display bands at 1559–1598; 1488–1565 and 1002–1060 cm^{-1} for the $\nu_{C=O}$, $\nu_{C=C}$ and ν_{C-S} vibrations, respectively, diagnostic of coordinated β -oxodithioester ligands.¹³ In the 1H NMR spectra of the ligands L1–L8, the $-OH$ protons at δ 14.62–15.37 ppm are absent in the complexes **1–8** due to keto–enol tautomerism. The position of the vinylic proton in the free ligands at δ 6.47–6.90 ppm and complexes at δ 6.45–7.21 ppm remains almost unchanged. A comparison of the 1H NMR spectra of

the methyl hydrogen atoms (–SMe) in **1**, **2**, **5**, **6**, and **7b**; aromatic protons in **3**, **4**, **6**, and **7a**; and anthracene ring protons in **5** with those observed in the parent ligands revealed no noticeable shift in the corresponding protons. This observation indicates that the Tl...H–C intermolecular anagostic interactions detected in the solid state from X-ray crystallography (*vide infra*) do not persist in solution. The $^{13}\text{C}\{^1\text{H}\}$ NMR resonances observed at δ 159.37–170.18 ppm for the C–OH carbon in the free ligands are not observed in the complexes due to stabilization of the keto form. The vinylic carbon of the ligands showed a chemical shift in the δ 106.56–108.26 ppm range; exceptionally in L5 the anthracene group is out of plane and therefore acts as an electron withdrawing group, showing a higher downfield shift of δ 115.17 ppm, while the corresponding vinylic carbon in the complexes at δ 111.08–116.37 ppm displays a downfield shift in the range δ 4.52–6.12 ppm. The –C=S carbon located at δ 215.92–219.27 ppm in the free ligands is upfield shifted at δ 193.34–198.92 ppm in the complexes indicating metal–ligand bonding. The –C=O carbon observed at δ 159.37–170.18 ppm in the ligands is located at δ 169.08–177.83 ppm in the complexes showing –C=O oxygen coordination.¹³ This indicates that the keto form of the β -oxodithioester ligands is stabilized in these complexes, as confirmed by the crystal structures *vide infra*, instead of the more stable enolate form reported in the transition metal complexes.¹³

Circular dichroism

Complexes **1** and **2** crystallized in chiral space groups; hence their CD spectra were studied in DMSO solution. The CD spectra of **1** and **2** show several deflections in the range of 386–430 nm as depicted in Fig. 1. The chirality of these complexes probably originates from their asymmetric arrangement about the metal center and/or the arrangement of monomeric units in the left and right handed helical motifs in **1** and **2**, respectively.²⁰ (See the crystal structure discussion *vide infra*.) The chiral nature of these compounds was further established using solid state CD spectra. As depicted in the ESI as Fig. S5,‡ the solid state CD spectra for **1** and **2** exhibited prominent dichroic signals at 384 and 310 nm respectively.

Absorption and emission spectra

The UV-Vis absorption spectra of complexes **1–8** in DMSO solution and as solid in nujol mull show virtually similar fea-

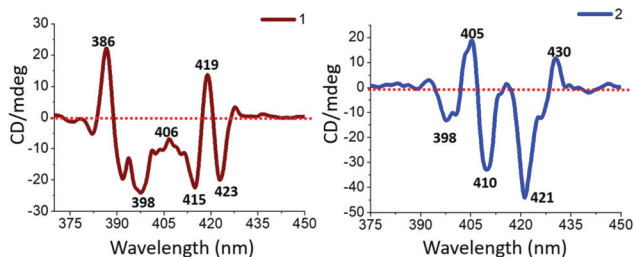


Fig. 1 CD spectra of complexes **1** and **2** in DMSO.

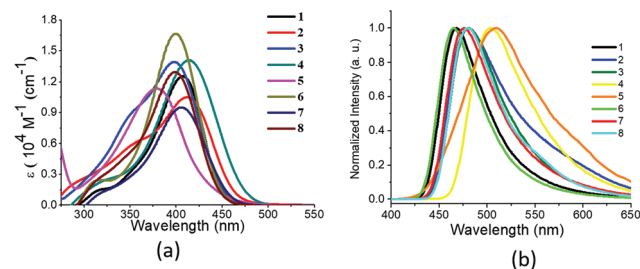


Fig. 2 (a) UV-Vis absorption and (b) fluorescence spectra of complexes **1–8** in DMSO.

tures (Fig. 2a and Fig. S2a, ESI‡). In solution, the absorption bands near 320–340 nm ($\epsilon = 2.85 \times 10^3$ – $6.24 \times 10^3 \text{ M}^{-1} \text{ cm}^{-1}$) and 380–425 nm ($\epsilon = 1.14 \times 10^4$ – $1.42 \times 10^4 \text{ M}^{-1} \text{ cm}^{-1}$) in all the complexes are assigned to intraligand charge transfer (ILCT) and metal perturbed ILCT transitions, respectively.^{21,22} The presence of an additional weak broad absorption band at 500 nm in **1–8** originates most likely from Tl...Tl interactions. This band is absent in the solution spectra thereby indicating a lack of thalophilic interactions in the solution.

The Tl(i) compounds are important from the view point of their luminescent properties. Upon excitation at 380 nm in DMSO solution, complexes **1–8** show an unstructured green emission band in the range of 465–510 nm (Fig. 2b) with a Stokes shift of 100–145 nm arising from the metal perturbed ILCT state. When excited at 350 nm in the solid phase, all the complexes show two to three unstructured emission bands near 475 and 550 nm (Fig. S2b and 2c, ESI‡) emanating from the ILCT and metal perturbed ILCT states,^{8,21} respectively, because except for L5 and L6 the remaining ligands are non-emissive in solution. L5 having a highly conjugated anthracene moiety and L6 having a small and highly electronegative F atom in the phenyl ring increasing conjugation due to a mesomeric effect when excited at 360 and 380 nm, respectively, show an unstructured intense broad emission band near 450 nm originating from the ILCT state. A larger red shifted emission band observed near 550 nm with a Stokes shift of ~200 nm in the solid state may be ascribed to Tl...Tl intermolecular interactions²³ in the polymeric structures. Notably, the stronger luminescence characteristics of **5** both in solid and solution phases in comparison with the remaining complexes may be attributed to the anthracene functionality on the ligand which enhances the delocalization within the molecule.

Lifetime evaluation

The fluorescence decay lifetime spectra²⁴ (Fig. 3) were recorded at room temperature in solution ($\lambda_{\text{exc}} = 380 \text{ nm}$) and they revealed a triexponential curve for all the complexes except **5**. The mean lifetime for **5** is remarkably longer at 9.79 ns when compared with the remaining complexes which show τ_{m} values in the range of 1.33–6.26 ns (Table 1). This unique behavior of **5** is explained by the presence of a highly conjugated and bulky anthracene chromophore in the dithioester ligand moiety and short Tl...Tl interactions.

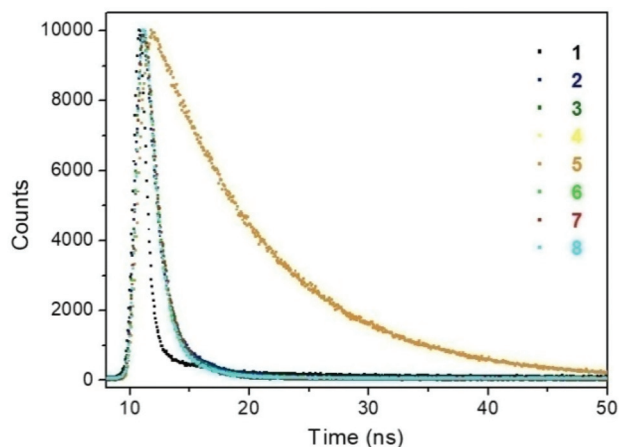


Fig. 3 Fluorescence lifetime decay profiles of 1–8 in DMSO at room temperature.

Table 1 Fluorescence decay lifetime data for complexes 1–8

Complex	τ_1 (α_1) ^a	τ_2 (α_2) ^a	τ_3 (α_3) ^a	τ_m ^b	χ^2
1	0.22 ns (68.95%)	33.59 ns (16.68%)	3.51 ns (14.37%)	6.26	1.13
2	0.95 ns (72.67%)	3.41 ns (21.10%)	14.16 ns (6.23%)	2.29	1.15
3	1.07 ns (81.91%)	2.93 ns (13.94%)	10.67 ns (4.15%)	1.73	1.13
4	0.84 ns (68.75%)	2.28 ns (25.32%)	9.78 ns (5.93%)	1.73	1.07
5	10.21 ns (83.30%)	7.71 ns (16.70%)	—	9.79	1.18
6	0.97 ns (81.10%)	4.36 ns (9.88%)	38.76 ns (9.02%)	4.71	1.16
7	1.02 ns (78.38%)	2.27 ns (19.48%)	10.11 ns (2.13%)	1.46	1.22
8	0.83 ns (70.93%)	1.98 ns (27.17%)	10.83 ns (1.90%)	1.33	1.09

^a α_i is the amplitude for the fluorescence lifetime τ_i . ^b The mean lifetime (τ_m) is calculated using the equation $\tau_m = \sum \alpha_i \tau_i$. τ is reported in ns.

Diffuse reflectance spectra

The optical band gaps for 1–8 were determined using solid state diffuse reflectance spectra (DRS) recorded against BaSO₄ as the reference at ambient temperature (Fig. 4a). The DRS shows that the studied complexes partly reflect the wavelengths in the studied region, particularly up to ca. 700 nm which suggests that the corresponding energies are being used by the complexes for excitation of electrons from the valence to conduction bands. The band gaps were calculated by using Planck's relationship, $E_{\text{band gap}} = hc/\lambda$, where h is Planck's constant ($4.135667516 \times 10^{-15}$ eV s), c is the velocity of light (2.998×10^8 m s⁻¹) and λ is the wavelength (nm). The suitable wavelength for band gap determination was ascertained using the first differential of the diffuse reflectance spectra (Fig. 4b).^{12c,13d,25} Complexes 1–8 show optical band gaps of 2.16, 2.26, 2.04, 2.15, 2.16, 2.11, 2.16 and 2.15 eV, respectively.

These values are in good agreement with the values derived from Kubelka–Munk functions²⁶ using the software package available with a Shimadzu UV-3101PC spectrometer (Fig. 4c). Optical band gaps in the range of 2.04–2.26 eV for the studied compounds suggest the semiconductor behavior of complexes^{27a–d} which is further supported by temperature dependent pressed pellet conductivity measurements.^{27e,f} The conductivities of all compounds range from 1.26×10^{-7} S cm⁻¹ to 9.55×10^{-7} S cm⁻¹ at room temperature (308 K). A steady increase in the conductivity was observed with the increase in temperature as depicted in Fig. S4 (ESI[†]).

Crystal structures

Single crystals of 1–8 were obtained by slow evaporation of the solutions of compounds in DMF within a week and those of ligand L5 and 7a were obtained in dichloromethane solutions within two weeks. Crystallographic data and structure refinement details for all crystals are given in Table S1 (ESI[†]) and selected bond distances and angles of 1–8 are given in Tables S2–S5 (ESI[†]).

The ORTEP diagram of L5 is presented in Fig. 5. The structure consists of two planar parts, the anthracene substituent (atoms C(21) to C(34)) and atoms O(11) to C(17) show r.m.s. deviations of 0.014 and 0.014 Å, respectively, and intersect at an angle of 68.77(3)°. The ligand is in the enol form forming intramolecular hydrogen bonds, O(11)–H...S(15), with O–H, S...H and O...S distances of 0.82(2), 2.15(2) and 2.926(12) Å, respectively, with a \angle O–H...S of 158(2)°.

The structures of complexes 1–8 contain Tl atoms with a wide variety of bonding patterns. It is often difficult to assess the nature of the coordination spheres because of the wide range of bond lengths around the metal. Donor atoms within 3.5 Å of the metal are considered to be within the coordination sphere but where it was thought relevant other atoms were also considered. In addition to bonds to O and S, all structures contained Tl...H contacts of note and these are considered together in a separate section. Complexes 1, 2, 3, 4, 7b and 8 contained one TIL moiety in the asymmetric unit with dimensions compared in Table S2 (ESI[†]). Complexes 5, 6 and 7a contained 2, 2, and 3 TIL moieties in the asymmetric unit with dimensions shown in Tables S3, S4 and S5 (ESI[†]) respectively.

The asymmetric units of complexes 1 and 2 derived from the β -oxodithioester ligands L1 and L2 having furyl and thienyl substituents on the dithioester unit contains only one formula unit (ORTEP diagram of 1 in Fig. 6).

It is noteworthy that complexes 1 and 2 crystallize in monoclinic and orthorhombic systems with $P2_1$ and $P2_12_12_1$ chiral space groups, respectively. Such non-centrosymmetric chiral space groups have been rarely found in Tl(i) complexes.²⁰ It is worth noting that the cell dimensions of 1 and 2 are very similar apart from the fact that the c axis in 2 is doubled in length. The chirality is a result of solid state packing in both structures given the fact that all starting compounds are achiral.

In both 1 and 2, while the asymmetric unit contains just one ligand and one metal, in both structures the metal atom is

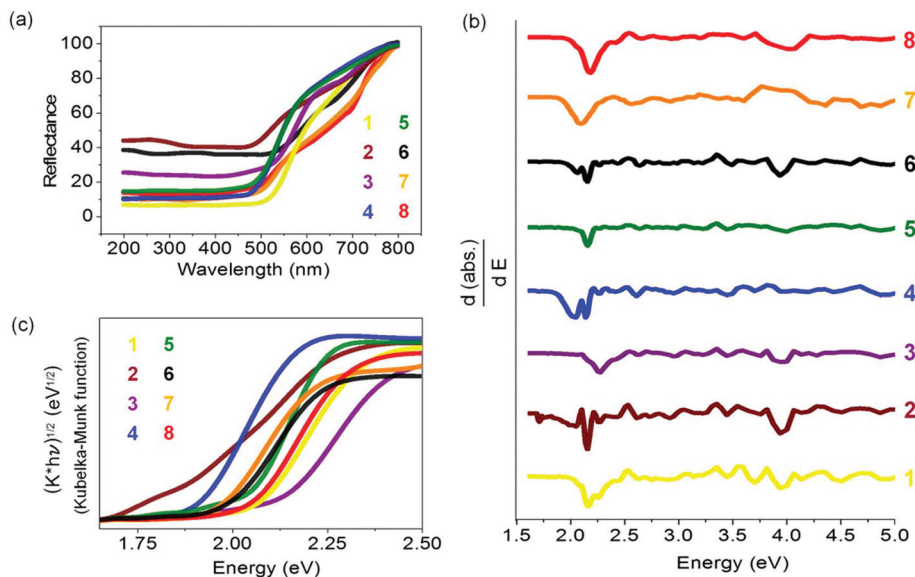


Fig. 4 (a) Diffuse reflectance plots for solids 1–8 at room temperature using BaSO₄ as the reference, (b) differentials of solid state absorbance of complexes with respect to radiation energy inflection points which give the band gap values and (c) Kubelka–Munk function vs. energy plot for complexes 1–8.

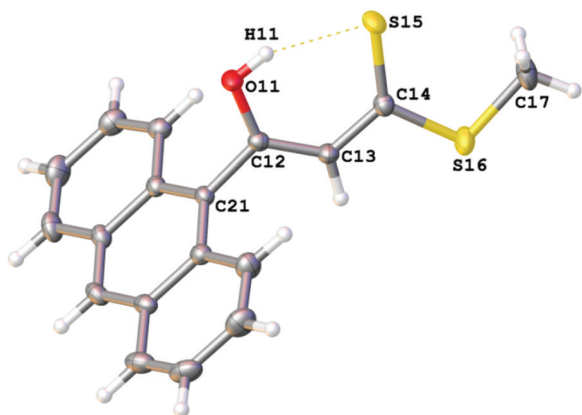


Fig. 5 X-ray crystal structure of ligand L5 with ellipsoids at 50% probability showing the atom numbering scheme. Hydrogen bond is shown as a dotted line.

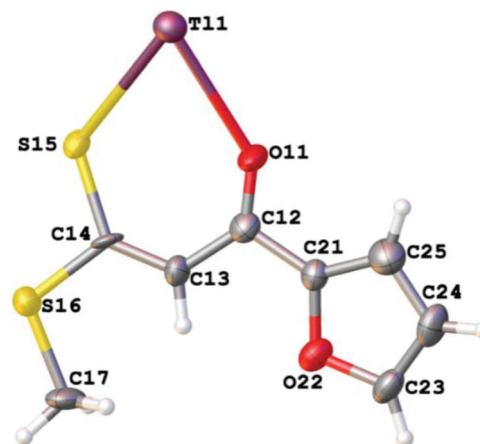


Fig. 6 The asymmetric unit of 1 with ellipsoids at 50% probability showing the atom numbering scheme. Complexes 2–4, 7b and 8 have similar asymmetric units.

seven-coordinated with a capped trigonal prismatic geometry being bonded to five sulfur atoms and two oxygen atoms from four different ligands. Thus in **1** the metal is chelated *via* O(11) and S(15) of the bidentate ligand to two ligands, and also *via* S(15) and S(16) from a third ligand and the coordination is completed by S(15) from a fourth ligand, the latter occupying a unique capping position; this arrangement is illustrated in Fig. 7a. Despite the differences in space groups, the arrangements around the metals are very similar although the symmetry elements involved are perforce different and indeed the dimensions are remarkably similar as clearly shown in Table S2 (ESI[†]). We discuss in detail here the dimensions in complex **1**. It is interesting to note that of the two ligands chelating through O(11) and S(15), one with shorter

bond lengths of 2.795(12) and 3.109(4) Å and a bite angle of 65.2(3)° shows the metal at 1.00(3) Å from the chelate plane, while the other ligand (symmetry operation: $-1 + x, y, z$) with dimensions of 3.271(17) and 3.191(5) Å and a bite angle of 59.2(3)° shows the metal at 2.77(1) Å; so the bonds are almost perpendicular to the chelate ring. A third bidentate interaction is found from S(15) and S(16) (symmetry operation: $(1 - x, \frac{1}{2} + y, -z)$) with T1–S distances of 3.273(4) and 3.413(5) Å and a bite angle of 50.6(1)°. An additional bond is found for S(15) ($1 - x, \frac{1}{2} + y, -z$) at 3.365(4) Å. There is also an interaction with a methyl hydrogen atom H(17A) ($-1 + x, 1 + y, z$) from a fifth ligand at 3.33 Å as shown in Fig. 7a. In the two structures the closest T1...T1 distances are 4.203(1) and 4.152(1) Å.

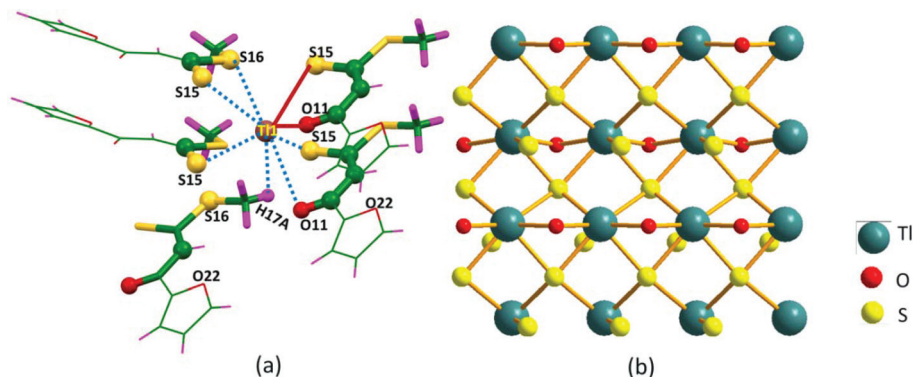


Fig. 7 (a) Coordination environment in **1** formed by Tl–O and Tl–S bonding and Tl...H–C intermolecular anagostic interactions and (b) 2D net-like coordination polymeric structure of **1**; Tl...H–C anagostic interactions have been omitted for clarity. Complex **2** shows a similar structure.

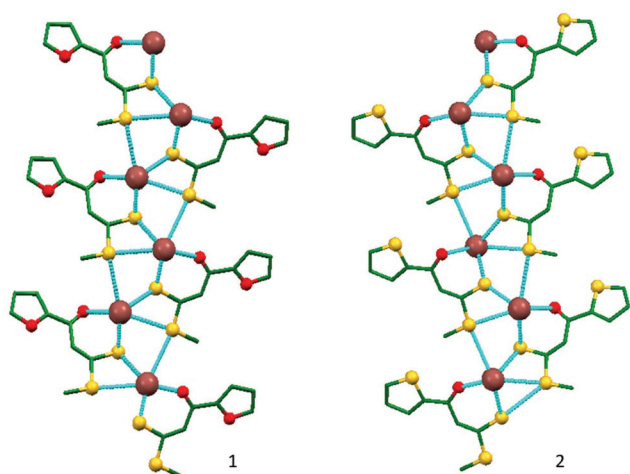


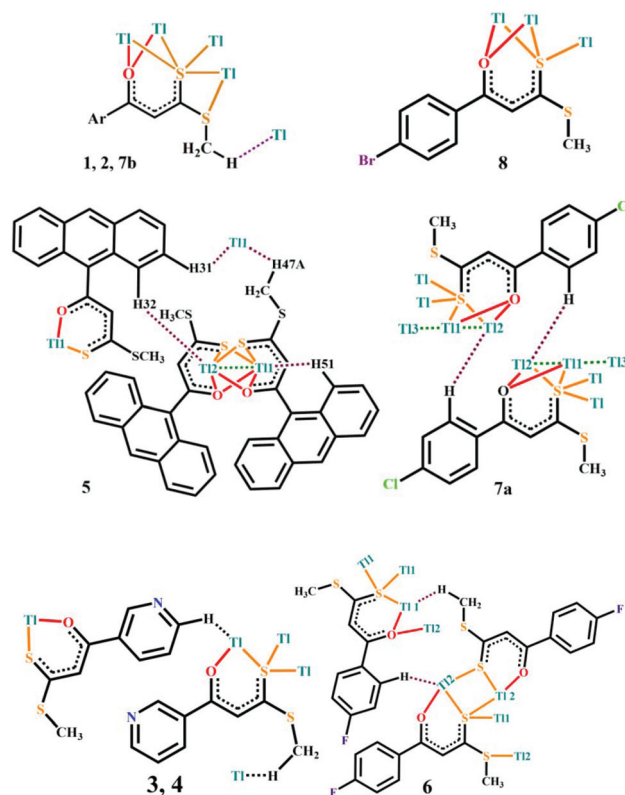
Fig. 8 Formation of helical motifs along the *b* axis in **1** and **2** sustained via bonding intermolecular interactions leading to chirality in their supramolecular architectures.

As shown in Fig. 8, the monomeric units in **1** and **2** form left and right handed helical^{20a} motifs sustaining several bonding intermolecular interactions.

In complexes **3** and **4** the cell dimensions are very similar but the space groups *Pccn* and *Iba2* are very different. In both cases, the asymmetric unit consists of only one molecule. The ORTEP diagrams for **3** and **4** are similar to that in Fig. 6. In **3** the metal is five-coordinate bonded to one oxygen and four sulfur atoms in a coordination environment best considered as a pentagonal bipyramid with one axial and one equatorial site missing. Thus, the py(N) atoms in position 3 in the β -oxodithioester ligand L3 is not involved in bonding to the metal despite its strong donor character presumably because of less flexibility of the pyridyl group directly attached to the dithioester unit. However, it is involved in several inter- and intramolecular interactions such as C–H...N and C–H...O.

The equatorial plane in **3** is occupied by two donor atoms from each of the two ligands; atoms O(11) and S(15) at 2.724 (3) and 2.893(1) Å, respectively, form a six-membered ring

together with S(15) and S(16) (symmetry element: $\frac{1}{2} - x, \frac{1}{2} - y, z$) forming a four membered ring with distances 3.187(1) and 3.590(1) Å, respectively. The r.m.s. deviation of this TlS₃O moiety in the equatorial plane is 0.053 Å. The unique bond to S(15) ($\frac{1}{2} - x, y, \frac{1}{2} + z$) in an axial position has a length of 3.024(1) Å. This axial S(15) atom bridges two Tl(1) atoms with a \angle Tl–S–Tl of 111.4(4)° in a $\mu_3\kappa^3$ -tridentate coordination mode (Scheme 3) on the adjacent molecules forming a 1D open



Scheme 3 Structural representation of complexes **1**–**8** showing Tl...Tl, Tl...H–C, chelating and chelating-bridging (μ_2 , μ_3 and μ_4) modes of coordination.

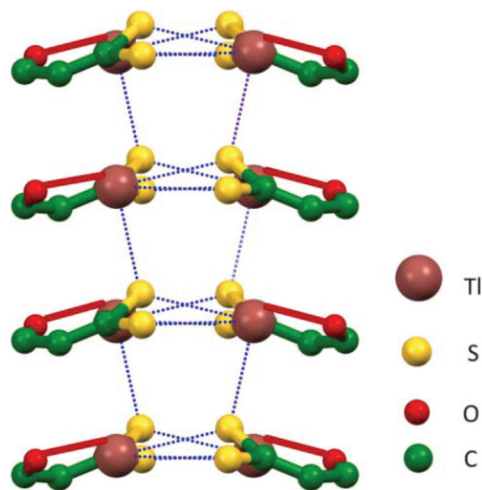


Fig. 9 1D open ladder-like coordination polymeric structure of **3** formed by the Tl–S intermolecular bonding. A similar polymeric structure is formed in **4**.

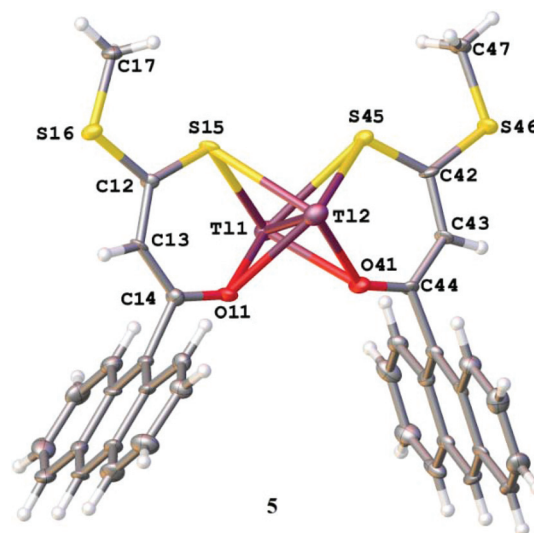


Fig. 10 The asymmetric unit of **5** with ellipsoids at 50% probability showing the atom numbering scheme.

ladder-like structure (Fig. 9). S(15) is therefore axial to one Tl and equatorial to the other.

The arrangement in **4** is similar but the Tl(1)–S(16) distance is significantly longer at 3.813(3) Å and there is a weak interaction with a second oxygen atom O(11) at 3.382(8) Å. This latter interaction is not observed in **3** where the distance is 4.666(9) Å.

Both structures contain two Tl...H–C contacts, one to a methyl hydrogen atom on C(17) at distances of 3.43 and 3.44 Å in approximately axial positions and another to the aromatic hydrogen atom H(24) in **3** and H(25) in **4** at 3.34 and 3.39 Å, respectively (Fig. 18).

The crystallographic asymmetric unit of **5** comprises two independent Tl(1) and Tl(2) atoms which are connected to each other at 3.724(5) Å forming a dimeric [TlL5]₂ unit showing significant thalophilic interactions.^{8,28–30} Both metals are chelated by two L5 ligands in the arrangement shown in Fig. 10. The distances shown in Table S3 (ESI[†]) are within the expected range.^{8,29,30} Both Tl atoms show one short Tl–O bond (2.651(5) and 2.572(5) Å) and one long Tl–O bond (2.848(5) and 2.904(6) Å) though the Tl–S distances fall within a narrow range of 2.943(3)–3.086(2) Å.

This structure is the only one of the eight Tl complexes that can be considered to be non-polymeric. Introduction of the bulky anthracenyl substituent on the dithioester backbone obstructed the involvement of O(15), O(45) and S(11), S(41) atoms in the formation of a coordination polymeric structure through effective Tl–O and Tl–S bonding thus imposing the low coordination numbers in **5** compared to those found in the other complexes. However, in addition to these four bonds, each Tl atom has an additional weak interaction with a sulfur atom S(45) for Tl(1) at 3.511(2) Å and S(16) for Tl(2) at 3.557(2) Å forming a 1D polymeric chain structure (Fig. 11). The closest inter-dimer Tl(1)···Tl(1) and Tl(2)···Tl(2) distances

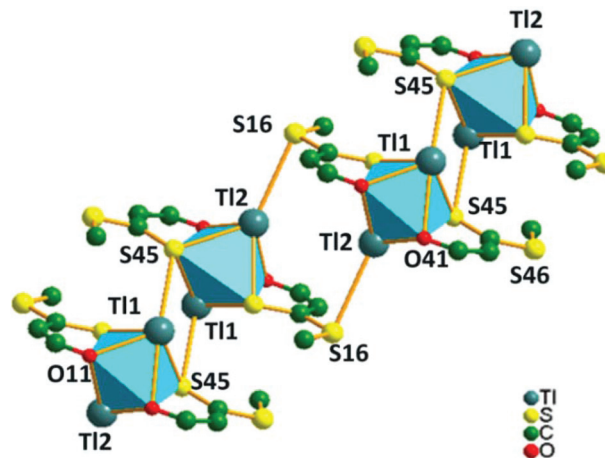


Fig. 11 The 1D polymeric chain structure of **5** formed through Tl(1)···S(45) and Tl(2)···S(16) contacts between the [Tl(1)Tl(2)(L5)₂] dimers.

of 4.356(1) Å and 4.348(1) Å are too long to indicate thalophilic interactions.

Complexes **6**, **7a**, **7b** and **8** derived from the dithioester ligands L6, L7 and L8 containing F, Cl and Br substituents at the *para* position of the phenyl ring, respectively, display distinctly different crystal packing and structural features because of their different sizes and electronegativities.

The asymmetric unit of **6**, dimensions shown in Table S4 (ESI[†]), contains two TlL moieties (Fig. 12). The distance between the two independent Tl(1) and Tl(2) atoms is 4.098(1) Å showing only weak thalophilic interaction. The arrangements around the two metals are very different: Tl(1) is bonded to one OS chelate, two SS chelates and an additional –SMe moiety while Tl(2) is bonded to two OS chelates and two sulfur atoms from different ligand molecules. Thus the O(11)

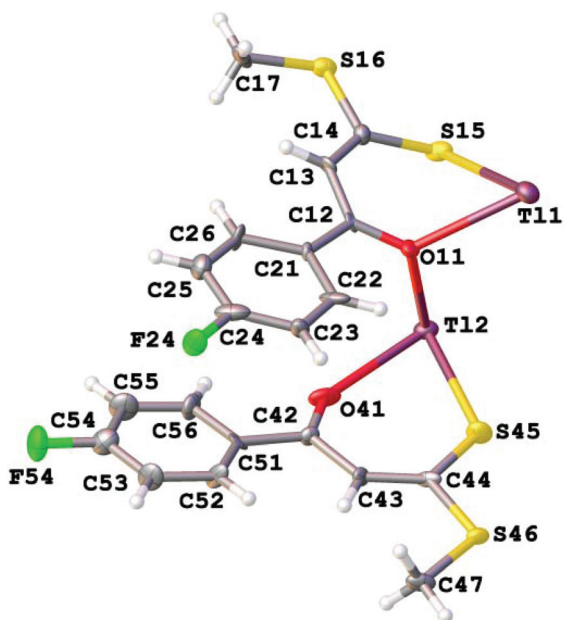


Fig. 12 The asymmetric unit of **6** with ellipsoids at 50% probability showing the atom numbering scheme.

and S(15) chelate is bonded to both metal atoms as follows: Tl(1)–O(11) (2.596(10) Å) and Tl(2)–O(11) (2.732(9) Å), and Tl(1)–S(15) (3.059(4)) and Tl(2)–S(15) (3.562(3) Å). A second ligand chelates Tl(2) with Tl(2)–O(41) with a distance of 2.840(12) and Tl(2)–S(45) with a distance of 2.998(3) Å. An additional atom S(45) also bridges Tl(1) and Tl(2) with distances of 3.266(4) and 3.209(4) Å. The asymmetric unit follows the $\mu_3\kappa^3$ -tridentate coordination mode forming a 2D polymeric structure (Fig. 13); the bridging Tl–S distances are significantly longer than that of the chelating O(41) as it is not involved in bridging but instead forms C–H...O hydrogen bonds at 2.45 Å. But Fig. 13 shows that S(15) primarily bridges Tl(1) atoms. It is to be noted that the fluorine atom at the *para* position of the benzene ring forms C–H...F intermolecular hydrogen bonds at

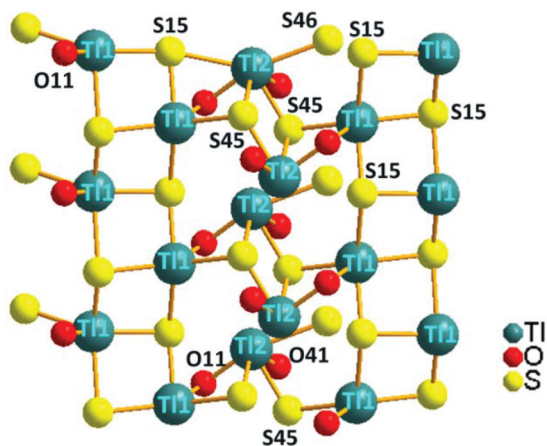


Fig. 13 2D polymeric structure of **6** formed by Tl–O and Tl–S bonds.

2.57–2.63 Å which is at the limit of hydrogen bonding behavior.

Remarkably when complex **7** is recrystallized from dichloromethane, crystals of **7a** are obtained which have a distinctly different structure from **7b**. The crystallographic asymmetric unit of **7a**, dimensions shown in Table S5 (ESI[†]), contains three independent Tl(1), Tl(2) and Tl(3) atoms (Fig. 14). The closest Tl(1)⋯Tl(2) and Tl(1)⋯Tl(3) intermetallic distances at 3.891(1) Å and 3.767(1) Å, respectively, are well within the range for thalophilic interactions.^{8,28–30} The two L7 ligands having a Cl substituent chelate Tl(1) and Tl(2) through O(51), S(55) and O(11), S(15) at 2.760(14), 3.241(4) Å and 2.629(12), 3.137(4) Å, respectively. S(15) and S(55) simultaneously bridge one Tl(1) and two Tl(3) atoms at 3.424(4), 3.139(4), and 3.297(4) Å and one Tl(1) and two Tl(2) atoms at 3.241(4), 3.283(4), and 3.371(4) Å, respectively. Furthermore, O(11) bridges Tl(2) and Tl(3) at 2.629(12) and 3.031(12) Å and O(31) bridges Tl(3) and Tl(1) at 3.008(11) and 2.794(12) Å, respectively, resulting in the formation of a 2D coordination polymeric structure showing the most spectacular arrangement of Tl atoms in a wave-like fashion (Fig. 15). The aromatic hydrogen at the *ortho* position H(23) of the benzene ring is involved in the rare Tl(2)⋯H–C intermolecular anagostic interactions (Fig. 18). Tl(1) and Tl(3) have no Tl⋯H interactions, and indeed they are the only thallium atoms in all the complexes **1–8** that have no such interactions.

In the structure of **7b**, there is only one TlL moiety in the asymmetric unit. The O and S atoms of ligand L7 coordinate in $\mu_2\kappa^2$ -bidentate chelating/bridging and $\mu_4\kappa^4$ -tetradentate chelating/bridging modes, respectively, resulting in a net-like 2D coordination polymeric structure (Fig. 16). The chelating and bridging Tl–O and Tl–S distances at 2.87(3)–3.00(3) Å and 3.108(11)–3.306(10) Å, respectively, are within the range mentioned in the literature.^{8,29,30}

The asymmetric unit of **8** also contains only one formula unit. Here, the coordination number around Tl is increased to 8 when Tl⋯H–C anagostic interactions are considered. L8 is coordinated to the Tl atom *via* O(11) and S(15) donor atoms in a $\mu_2\kappa^2$ -bidentate and $\mu_3\kappa^3$ -tridentate manner (Scheme 3), sim-

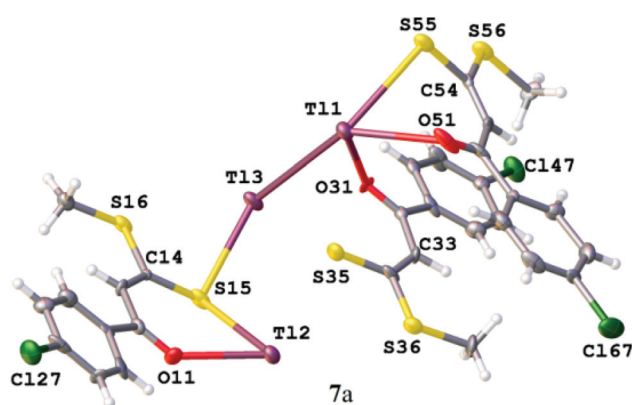


Fig. 14 The asymmetric unit of **7a** with ellipsoids at 50% probability showing the atom numbering scheme.

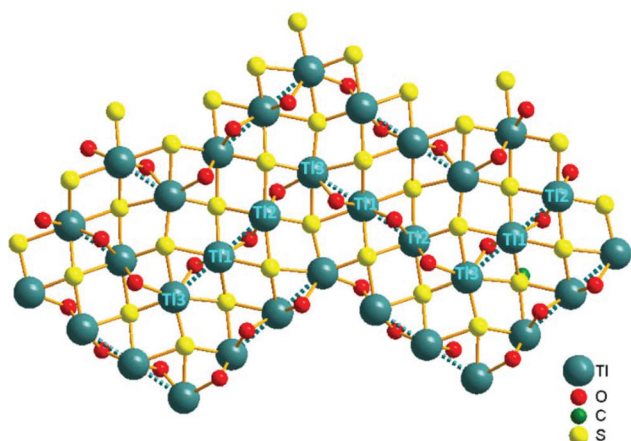


Fig. 15 2D coordination polymeric structure formed by Tl–O and Tl–S bonds showing a wave-like arrangement of Tl atoms in **7a**.

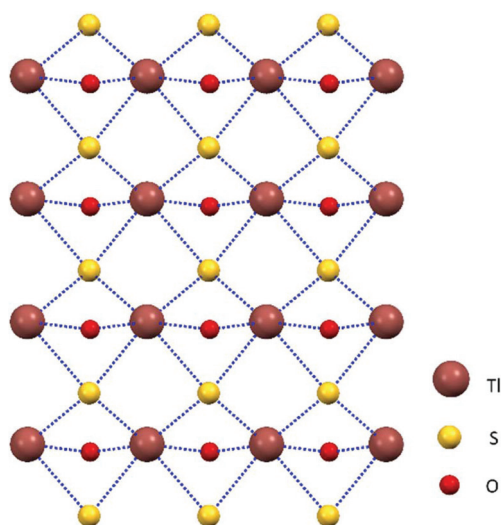


Fig. 16 2D net-like coordination polymeric structure of **7b** formed by Tl–O and Tl–S bonds; interactions are included. However, in this figure H atoms are omitted for clarity.

ultaneously chelating one Tl(1) and bridging another neighbouring Tl(i), respectively. These chelating and bridging contacts lead to formation of a 1D coordination polymeric open ladder-like structure (Fig. 17). The difference between the polymeric structure of **8** and the 2D structures of **6** and **7** (having F and Cl substituents) may be attributed to the larger size and smaller electronegativity of the Br substituent at the *para* position of ligand L8. The closest Tl(1)⋯Tl(1) contact of 4.605(1) Å between the zig-zag chain of metal atoms with a \angle Tl(1)–Tl(1)–Tl(1) of 98.03(1)° shows a lack of metallophilic interaction. The chelating and bridging Tl–O and Tl–S distances at 2.869(16)–3.137(17) Å and 2.989(6)–3.115(6) Å, respectively, are well within the literature values,^{8,29,30} with the bridging distances longer than the chelating distances. An open ladder-like structure built on

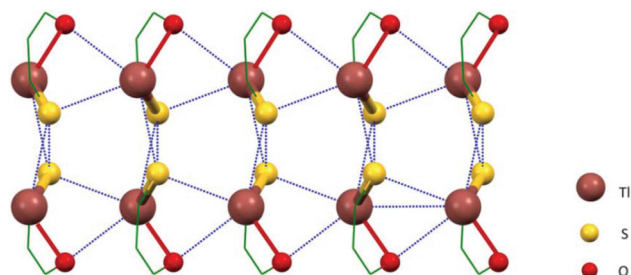


Fig. 17 Open ladder-like 1D coordination polymeric structure of **8** formed by Tl–O and Tl–S bonds. The Tl⋯H–C anagostic bond is omitted for clarity.

Tl–S and Tl–O inter- and intramolecular bonds is observed (Fig. 17).

1–8 are unique examples of Tl(i) complexes with (O, S) donor β -oxodithioester ligands exhibiting remarkable variations in their structures and bonding assisted by several interactions in their networks.

The term agostic bonding was used for a $3c-2e$ covalent bond formed where the C–H bond acts as a ligand to electron seeking transition metal ions.^{28,31} The rare preagostic or anagostic M⋯H–C bonding, largely electrostatic in nature, is observed in planar organometallic and metal dithiolates including dithiocarbamate complexes. Here, M = Ni(II), Pd(II), Pt(II), Cu(II) and Rh(I) metal ions with d^8/d^9 electronic configurations.³² The former is generally regarded to be mechanistically important for the key step in C–H activation processes³³ while the latter is recognized as a pre-stage to agostic bonding and of broad general interest due to possible implications for the mechanism of C–H activation.³³

The striking feature of complexes **1–8** is the existence of rare Tl⋯H–C intermolecular anagostic interactions in all structures. This interaction is facilitated by the fact that the coordination sphere around the metal of sulfur and oxygen atoms contains an empty site. Crystal packing effects in addition to steric and electronic properties of the substituents on the dithioester unit are elemental in bridging the hydrogen atom in close vicinity of the metal centre. For the structures with one metal in the asymmetric unit, namely **1**, **2**, **3**, **4**, **7b** and **8**, the Tl⋯H–C distances, are in the range 3.24 to 3.47 Å⁸ with Tl⋯H–C angles of 118–135° (details in Table S2, ESI†). These interactions involve a methyl hydrogen atom on C(17) and the hydrogen occupies a vacant approximately axial position in the metal coordination sphere. It is noted from Table S2 (ESI†) that in structures **3** and **4**, there is a second Tl⋯H interaction and this involves aromatic hydrogen atoms H(24) and H(25), respectively. Structures **5**, **6** and **7a** have two or more metal atoms in the asymmetric unit and the involvement of hydrogen atoms is necessarily more complicated. In **5** there are four protons around Tl(1), namely H(51), H(47A)\$1, H(21) and H(31)\$3, participating in anagostic interactions at 3.30, 3.23, 3.50, and 3.34 Å, respectively, and one around Tl(2), namely H(32)\$1, at a distance of 3.22 Å. It is noted that two of the anagostic interactions around Tl(1) are intramolecular in nature.

The Tl...H-C angles involving Tl(1) are in the range of 136–158° considerably larger than that involving Tl(2) at 122°.

Notably, these hydrogen atoms occupy coordination sites about the metal along with the closest donor atoms that are O(41) and S(45) atoms on the adjacent molecules in **5** and O(11) in both **6** and **7a** from dithioester ligands forming spectacular 7-, 11- and 12-membered chelate rings, respectively (Fig. 18).

In structure **6**, both of the independent thallium atoms have an interaction with hydrogen in an axial position, at 3.21 and 3.21 Å with Tl...H-C angles of 132 and 139°, respectively. Complex **7a** contains three metal atoms in the asymmetric unit but Tl(1) and Tl(3) are not in close contact with hydrogen

atoms. Tl(2) has just one such interaction with H(23) at 3.25 Å with an angle of 148°. These rare Tl...H-C intermolecular anagostic interactions are illustrated in Fig. 18.

Considering these interactions as bonding, the effective coordination number about the metal center in these complexes is enhanced. The Tl...H distances in these complexes are somewhat longer than those found at 2.61–2.89 Å in Ni(II), Pd(II), Pt(II) and Cu(II) dithiocarbamate complexes³² but are well within the range of values of previously reported Tl(I) dithiocarbamate complexes.⁸ This may be ascribed to the larger size, high relativistic effects and stereochemically active lone pair on the Tl(I) ion. The observed anagostic interactions

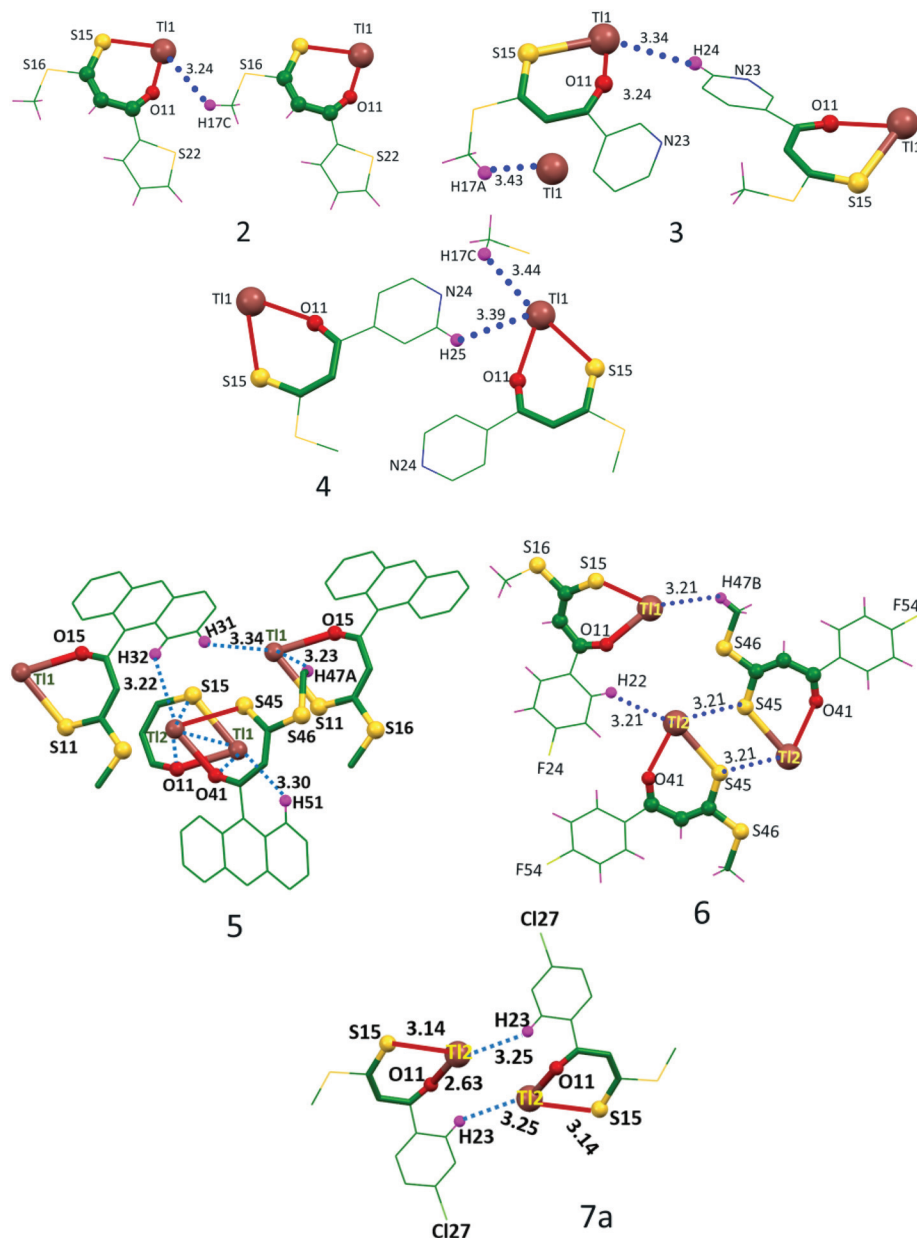


Fig. 18 Depiction of Tl...H-C intermolecular anagostic interactions in complexes **2**, **3** and **4**. Complexes **1**, **7b** and **8** show interactions similar to **2**. The formation of chelate rings around the Tl atom in **5**, **6** and **7a** shows Tl...H-C intermolecular anagostic interactions.

in these complexes are in the order $6 > 5 > 2 > 7a > 1 > 3 > 4 > 7b > 8$.

Single point calculations were carried out to assess the energy of these Tl...H-C anagostic interactions. For **1** and **2**, we used two TIL asymmetric units connected by a simple translation and connected *via* Tl...H(methyl) interactions. Calculations using the formula Energy of dimer = 2 × monomer yielded the values -2.46 and -2.34 kcal mol⁻¹. Similar calculations on **7b** gave an energy difference of -0.74 kcal mol⁻¹.

Apart from these direct Tl...H-C anagostic interactions, hydrogen atoms play an important role in generating C-H... π (MS₂C, chelate) interactions. Tiekink and Zuckerman-Schpector have described³⁴ the important role of such interactions in transition and main group metal 1,1-dithiolates in facilitating the construction of multi-dimensional supramolecular architectures.³⁵ The structural features of this kind of interaction were defined by three dimensions, α the angle between the perpendicular to the ring and the H...CG vector (CG being the centroid of the four-membered MS₂C ring), β the CG...H-C angle and d the H...CG distance. The examples with values of $\alpha < 20^\circ$, β in the range of 110 – 180° and d between 2.4 and 3.6 Å were found to define the C-H... π (MS₂C, chelate) interactions of interest. The existence of such interactions in the main group metal complexes is less commonly observed as compared to transition metal complexes because of the lack of planarity.^{12,34} The stereochemically active 6s² lone pair with greater relativistic contribution of the Tl atom and formation of a highly delocalized 6-membered ring about the metal center in **5** together with crystal packing effects, notably exhibits C-H... π (TIOSC₃, chelate) interactions (Fig. 19). It is to be noted that in **5** intramolecular interactions between hydrogen atoms of anthracene, H(21) with Tl(1) and H(61) with Tl(2), are observed with α , β and d values of 1° , 132° , 2.96 Å and 8° , 129° , 3.21 Å, respectively.

Furthermore, the coordination polymeric structures of complexes **1**–**8** were supported by important non-covalent interactions, H...H, C-H... π , C-H... π (TIOSC₃, chelate), Tl...H-C anagostic and C-H...X (X = N, O, F and Cl) hydrogen bond interactions³⁵ sustaining the multi-dimensional architecture of the complexes (Fig. S2.1–S2.2 and Table S6, ESI†).

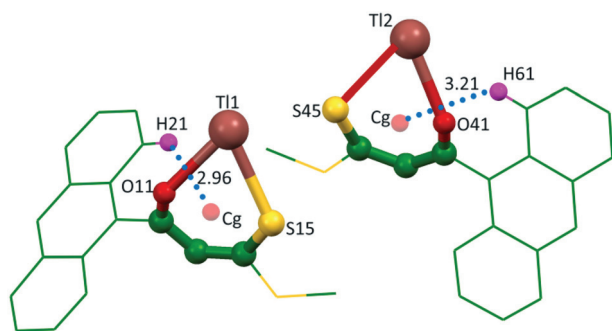


Fig. 19 Representation of C-H... π (TIOSC₃, chelate) interactions in **5**.

Conclusions

Eight new β -oxodithioester Tl(i) complexes were synthesized and fully characterized. These provide efficient examples of complexes which highlight the effect of steric and electronic properties of various substituents on the ligand backbone in the development of interesting solid state structures. **1**–**8** portray unprecedented 1D and 2D ladder/net-like coordination polymeric structures, interesting anagostic and C-H... π (TIOSC₃, chelate) interactions along with several other hydrogen bonding, covalent and non-covalent interactions. These interactions proved crucial in the formation of two (**1** and **2**) chiral Tl(i) complexes aligning as helices in their supramolecular structure. The β -oxodithioester ligands are bonded to the Tl(i) centers in (O, S) chelating and chelating-bridging μ_2 , μ_3 and μ_4 modes (Scheme 3). The structure of **7a** is most intriguing as it contains three independent thallium atoms uniquely linked with each other forming a 2D wave-like polymeric structure. **5**, **6** and **7a** exhibited 7-, 11-, and 12-membered chelate rings *via* (H, O, S) bonding and anagostic interactions about the metal center. These anagostic interactions were assessed by theoretical calculations. Compared with the case of Tl(i) dithiocarbamates, identical (S, S) donor atoms forming strained 4-membered chelate rings bond in the chelating-bridging mode in the formation of a dimeric unit but not in a bridging fashion in the coordination polymeric structures. All the complexes show bright green fluorescence emission in the solution and solid phases at room temperature originating from the metal perturbed intra-ligand charge transfer states and Tl...Tl interactions. Particularly, the stronger luminescence characteristics of **3**, **4** and **5** are due to the presence of higher conjugation in the pyridyl and anthracene moieties of the substituents and conformational rigidity in the extended polymeric structures. The fluorescence lifetime of **5** is significantly higher than that of the remaining complexes due to greater steric bulk of the anthracene chromophore and the shorter Tl...Tl distance. DRS and temperature dependent pressed pellet conductivity measurements indicate the semiconducting behavior of complexes **1**–**8**. This study extends the scope of coordination polymers derived from thallium metal with dithioester ligands for their intriguing structural features and possible applications as luminescent and semiconducting materials.

Conflicts of interest

There are no conflicts to declare.

Acknowledgements

We gratefully acknowledge financial support from the Science and Engineering Research Board (SERB) for the project: (SB/SI/IC-15/2014) and University Grants Commission (UGC), New Delhi for the award of BSR Faculty Fellow (ref No. F.18-1 (BSR) 30 Dec 2016) to NS and UGC-SRF fellowship to CLY. GR

acknowledges Department of Science and Technology (DST), New Delhi for DST-INSPIRE Faculty fellowship (award ref no. DST/INSPIRE/04/2016/000997). We are also thankful to Department of Chemistry, Institute of Science, Banaras Hindu University, UGC CAS-II for infrastructural facilities and University of Reading, EPSRC (UK) for funds for the diffractometer used in the data collection of samples L5, 2 and 5-8.

Notes and references

- M. P. Suh, Y. E. Cheon and E. Y. Lee, *Coord. Chem. Rev.*, 2008, **252**, 1007–1026.
- O. M. Yaghi, M. Okeeffe, N. W. Ockwig, H. K. Chae, M. Eddaoudi and J. Kim, *Nature*, 2003, **423**, 705–714.
- N. W. Ockwig, O. Delgado-Friedrichs, M. Okeeffe and O. M. Yaghi, *Acc. Chem. Res.*, 2005, **38**, 176–182.
- A. K. Cheetham, C. N. R. Rao and R. K. Feller, *Chem. Commun.*, 2006, **46**, 4780–4795.
- T. R. Cook, Y. R. Zheng and P. J. Stang, *Chem. Rev.*, 2013, **113**, 734–777.
- F. Caruso, M. L. Chan and M. Rossi, *Inorg. Chem.*, 1997, **36**, 3609–3615.
- (a) S. K. Dutta and M. W. Perkovic, *Inorg. Chem.*, 2002, **41**, 6938–6940; (b) P. D. McNaughtner, S. A. Saah, M. Akhtar, K. Abdulwahab, M. A. Malik, J. Raftery, J. A. M. Awudza and P. O'Brien, *Dalton Trans.*, 2016, **45**, 16345–16353.
- (a) V. Kumar, V. Singh, A. N. Gupta, M. G. B. Drew and N. Singh, *Dalton Trans.*, 2015, **44**, 1716–1723; (b) K. K. Manar, G. Rajput, M. K. Yadav, C. L. Yadav, K. Kumari, M. G. B. Drew and N. Singh, *ChemistrySelect*, 2016, **1**, 5733–5742; (c) L. Nilson and R. Hesse, *Acta Chem. Scand.*, 1969, **23**, 1951–1965; (d) E. Elfving, H. Anacker-Eickhoff and R. Hesse, *Acta Chem. Scand., Ser. A*, 1976, **30**, 335–339; (e) A. V. Ivanov, O. A. Bredynk, A. V. Gerasimenko, O. N. Antzutkin and W. Forsling, *Russ. J. Coord. Chem.*, 2006, **32**, 339–349; (f) B. Krebs and A. Brommelhaus, *Angew. Chem., Int. Ed. Engl.*, 1989, **28**, 1682–1683.
- K. Ramasamy, V. L. Kuznetsov, K. Gopal, M. A. Malik, J. Raftery, P. P. Edwards and P. O'Brien, *Chem. Mater.*, 2013, **25**, 266–276.
- (a) N. O. Bodi, M. A. Malik, P. O'Brien and J. A. M. Awudza, *Dalton Trans.*, 2012, **41**, 10497–10506; (b) J. R. Casto, K. C. Molloy, Y. Liu, C. S. Lai, T. J. White and E. R. T. Tiekink, *J. Mater. Chem.*, 2008, **18**, 5399–5405.
- (a) D. Coucouvanis, *Prog. Inorg. Chem.*, 1970, **11**, 233–371; (b) D. Coucouvanis, *Prog. Inorg. Chem.*, 1979, **26**, 301–469; (c) G. Hogarth, *Prog. Inorg. Chem.*, 2005, **53**, 71–561; (d) G. Hogarth, *Mini-Rev. Med. Chem.*, 2012, **12**, 1202–1215; (e) E. R. T. Tiekink and I. Haiduc, *Prog. Inorg. Chem.*, 2005, **54**, 127–319; (f) P. J. Heard, *Prog. Inorg. Chem.*, 2005, **53**, 1–69.
- (a) A. Kumar, R. Chauhan, K. C. Molloy, G. K. Kohn, L. Bahadur and N. Singh, *Chem. – Eur. J.*, 2010, **16**, 4307–4314; (b) V. Singh, R. Chauhan, A. N. Gupta, V. Kumar, M. G. B. Drew, L. Bahadur and N. Singh, *Dalton Trans.*, 2014, **43**, 4752–4761; (c) G. Rajput, M. K. Yadav, M. G. B. Drew and N. Singh, *Inorg. Chem.*, 2015, **54**, 2572–2579.
- (a) R. Saumweber, C. Robl and W. Weigand, *Inorg. Chim. Acta*, 1998, **269**, 83–90; (b) I. G. Orozco, J. G. L. Cortes, M. C. O. Alfaro, R. A. Toscano, G. P. Carrillo and C. A. Toledano, *Inorg. Chem.*, 2004, **43**, 8572–8576; (c) I. G. Orozco, M. C. O. Alfaro, J. G. L. Cortes, R. A. Toscano and C. A. Toledano, *Inorg. Chem.*, 2006, **45**, 1766–1773; (d) G. Rajput, M. K. Yadav, M. G. B. Drew and N. Singh, *Dalton Trans.*, 2015, **44**, 5909–5916.
- A. W. M. Lee, W. H. Chan and H. C. Wong, *Synth. Commun.*, 1988, **18**, 1531–1536.
- M. J. Frisch, G. W. Trucks, H. B. Schlegel, G. E. Scuseria, M. A. Robb, J. R. Cheeseman, J. A. Montgomery Jr., T. Vreven, K. N. Kudin, J. C. Burant, J. M. Millam, S. S. Iyengar, J. Tomasi, V. Barone, B. Mennucci, M. Cossi, G. Scalmani, N. Rega, G. A. Petersson, H. Nakatsuji, M. Hada, M. Ehara, K. Toyota, R. Fukuda, J. Hasegawa, M. Ishida, T. Nakajima, Y. Honda, O. Kitao, H. Nakai, M. Klene, X. Li, J. E. Knox, H. P. Hratchian, J. B. Cross, V. Bakken, C. Adamo, J. Jaramillo, R. Gomperts, R. E. Stratmann, O. Yazyev, A. J. Austin, R. Cammi, C. Pomelli, J. W. Ochterski, P. Y. Ayala, K. Morokuma, G. A. Voth, P. Salvador, J. J. Dannenberg, V. G. Zakrzewski, S. Dapprich, A. D. Daniels, M. C. Strain, O. Farkas, D. K. Malick, A. D. Rabuck, K. Raghavachari, J. B. Foresman, J. V. Ortiz, Q. Cui, A. G. Baboul, S. Clifford, J. Cioslowski, B. B. Stefanov, G. Liu, A. Liashenko, P. Piskorz, L. Komaromi, R. L. Martin, D. J. Fox, T. Keith, M. A. Al-Laham, C. Y. Peng, A. Nanayakkara, M. Challacombe, P. M. W. Gill, B. Johnson, W. Chen, M. W. Wong, C. Gonzalez and J. A. Pople, *Gaussian 03, Revision C.02*, Gaussian, Inc., Wallingford CT, 2004.
- Oxford Diffraction, *CrysAlis CCD, RED, version 1.711.13, copyright (1995–2003)*, Oxford Diffraction Poland Sp.
- G. M. Sheldrick, SHELXS-97, *Acta Crystallogr., Sect. A: Found. Crystallogr.*, 2008, **A64**, 112–122.
- G. M. Sheldrick, *SHELXL2016–16, Program for Crystal Structure Refinement*, University of Gottingen, Gottingen, 1997.
- (a) O. V. Dolomanov, L. J. Bourhis, R. J. Gildea, J. A. K. Howard and H. Puschmann, *J. Appl. Crystallogr.*, 2009, **42**, 339–341; (b) K. Brandenburg, *DIAMOND Crystal Impact GbR*, Bonn, Germany, 1999; (c) C. F. Macrae, I. J. Bruno, J. A. Chisholm, P. R. Edgington, P. McCabe, E. Pidcock, L. Rodriguez-Monge, R. Taylor, J. van de Streek and P. A. Wood, *J. Appl. Crystallogr.*, 2008, **41**, 466–470.
- (a) G. M. Davies, J. C. Jeffery and M. D. Ward, *New J. Chem.*, 2003, **27**, 1550–1553; (b) E. Craven, E. Mutlu, D. Lundberg, S. Temizdemir, S. Dechert, H. Brombacher and C. Janiak, *Polyhedron*, 2002, **21**, 553–562.
- (a) E. J. Fernandez, A. Laguna, J. M. Lopez-de-Luzuriaga, M. Monge, M. Montiel, M. E. Olmos and J. Perez, *Organometallics*, 2004, **23**, 774–782; (b) M. V. Childress,

- D. Millar, T. M. Alam, K. A. Kreisel, G. P. A. Yap, L. N. Zakharov, J. A. Golen, A. L. Rheingold and L. H. Doerrer, *Inorg. Chem.*, 2006, **45**, 3864–3877; (c) F. Sabin and A. Vogler, *Monatsh. Chem.*, 1992, **123**, 705–708.
- 22 (a) E. J. Fernandez, A. Laguna and J. M. Lopez-de-Luzuriaga, *Coord. Chem. Rev.*, 2005, **249**, 1423–1433; (b) A. Strasser and A. Vogler, *Inorg. Chem. Commun.*, 2004, **7**, 528–530; (c) V. J. Catalano, B. L. Bennett and H. M. Kar, *J. Am. Chem. Soc.*, 1999, **121**, 10235–10236.
- 23 P. C. Ford and A. Vogler, *Acc. Chem. Res.*, 1993, **26**, 220–226.
- 24 (a) G. Krishnamoorthy, *J. Mol. Biol.*, 2009, **393**, 735–752; (b) D. G. Cuttall, S. M. Kuang, P. E. Fanwick, D. R. McMillin and R. A. Walton, *J. Am. Chem. Soc.*, 2002, **124**, 6–7; (c) M. K. Singh, H. Pal, A. S. R. Koti and A. V. Sapre, *J. Phys. Chem.*, 2004, **108**, 1465–1474; (d) D. M. Zink, T. Baumann, J. Friedrichs, M. Nieger and S. Brase, *Inorg. Chem.*, 2013, **52**, 13509–13520; (e) J. Pospisil, I. Jess, C. Nather, M. Necasa and P. Taborsky, *New J. Chem.*, 2011, **35**, 861–864.
- 25 A. E. Morales, E. S. Mora and U. Pal, *Rev. Mex. Fis. S.*, 2007, **53**, 18–22.
- 26 J. Tauc, R. Grigorovici and A. Vancu, *Phys. Status Solidi*, 1966, **15**, 627–637.
- 27 (a) X. Zhao, S. Zhang, J. Yan, L. Li, G. Wu, W. Shi, G. Yang, N. Guan and P. Cheng, *Inorg. Chem.*, 2018, **57**, 5030–5037; (b) Y. Liu, F. Wei, S. N. Yeo, F. M. Lee, C. Kloc, Q. Yan, H. H. Hng, J. Ma and Q. Zhang, *Inorg. Chem.*, 2012, **51**, 4414–4416; (c) T. Okubo, H. Anma, N. Tanaka, K. Himoto, S. Seki, A. Saeki, M. Maekawa and T. Karuda-Sowa, *Chem. Commun.*, 2013, **49**, 4316–4318; (d) P. I. Clemenson, *Coord. Chem. Rev.*, 1990, **106**, 171–203; (e) G. Rajput, V. Singh, A. N. Gupta, M. K. Yadav, V. Kumar, S. K. Singh, A. Prasad, M. G. B. Drew and N. Singh, *CrystEngComm*, 2013, **15**, 4676–4683; (f) G. Rajput, V. Singh, S. K. Singh, L. B. Prasad, M. G. B. Drew and N. Singh, *Eur. J. Inorg. Chem.*, 2012, **15**, 3885–3891.
- 28 (a) P. Pyykko, *Chem. Rev.*, 1997, **97**, 597–636; (b) C. Janiak, *Coord. Chem. Rev.*, 1997, **163**, 107–216; (c) C. H. Galka and L. H. Gade, *Inorg. Chem.*, 1999, **38**, 1038–1039.
- 29 (a) F. Wiesbrock and H. Schmidbaur, *J. Am. Chem. Soc.*, 2003, **125**, 3622–3630; (b) D. Marcano, N. Gerasimchuk, V. Nemykin and S. Silchenko, *Cryst. Growth Des.*, 2012, **12**, 2877–2889.
- 30 (a) H. Pritzkow and P. Jennische, *Acta Chem. Scand., Ser. A*, 1975, **29**, 60–70; (b) B. E. Bosch, M. Eisenhawer, B. Kersting, K. Kirschbaum, B. Krebs and D. M. Giolando, *Inorg. Chem.*, 1996, **35**, 6599–6605; (c) H. Schmidbaur, *Angew. Chem., Int. Ed. Engl.*, 1985, **24**, 893–1008.
- 31 (a) M. Brookhart, M. L. H. Green and G. Parkin, *Proc. Natl. Acad. Sci. U. S. A.*, 2007, **104**, 6908–6914; (b) H. V. Huynh, L. R. Wong and P. S. Ng, *Organometallics*, 2008, **27**, 2231–2237; (c) J. Sabmannshausen, *Dalton Trans.*, 2012, **41**, 1919–1923; (d) K. A. Siddiqui and E. R. T. Tiekink, *Chem. Commun.*, 2013, **49**, 8501–8503; (e) S. Scholer, M. H. Wahl, N. I. C. Wurster, A. Puls, C. Hattig and G. Dyker, *Chem. Commun.*, 2014, **50**, 5909–5911; (f) W. H. Bernskoetter, C. K. Schauer, K. I. Goldberg and M. Brookhart, *Science*, 2009, **326**, 553–556; (g) M. Stepien and L. Latos-Grazynski, *Acc. Chem. Res.*, 2005, **38**, 88–98; (h) M. Teci, E. Brenner, D. Matt, C. Gourlaouen and L. Toppr, *Dalton Trans.*, 2015, **44**, 9260–9268; (i) J. A. Harrison, A. J. Nielson, M. A. Sajjad, G. C. Saunders and P. Schwerdtfeger, *Eur. J. Inorg. Chem.*, 2016, 64–77.
- 32 (a) R. Angamuthu, L. L. Gelauff, M. A. Siegler, A. L. Spek and E. Bouwman, *Chem. Commun.*, 2009, **7**, 2700–2702; (b) B. Singh, M. G. B. Drew, G. K. Kohn, K. C. Molloy and N. Singh, *Dalton Trans.*, 2011, **40**, 623–631; (c) A. N. Gupta, V. Kumar, V. Singh, K. K. Manar, M. G. B. Drew and N. Singh, *CrystEngComm*, 2014, **16**, 9299–9307.
- 33 (a) W. Yao, O. Eisenstein and R. H. Crabtree, *Inorg. Chim. Acta*, 1997, **254**, 105–111; (b) J. L. Haller, M. J. Page, S. A. Macgregor, M. F. Mohan and M. K. Whittlesey, *J. Am. Chem. Soc.*, 2009, **131**, 4604–4605.
- 34 (a) E. R. T. Tiekink and J. Z. Schpector, *Chem. Commun.*, 2011, **47**, 6623–6625; (b) C. I. Yeo, S. N. A. Halim, S. W. Ng, S. L. Tan, J. Z. Schpector, M. A. B. Ferreira and E. R. T. Tiekink, *Chem. Commun.*, 2014, **50**, 5984–5986.
- 35 V. R. Thalladi, H. C. Weiss, D. Blaser, R. Boese, A. Nangia and G. R. Desiraju, *J. Am. Chem. Soc.*, 1998, **120**, 8702–8710.